EVALUATION OF THE BIOLOGICAL EFFECT SYNTHESIZED IRON OXIDE NANOPARTICLES ON *ENTEROCOCCUS FAECALIS*

R. M. kamel **L. A. Yaaqoob**
Researcher **Assist. Prof.**
Department of Biotechnology, Science College, University of Baghdad, Baghdad, Iraq
rahma.m.kamel@gmail.com **laith.yaaqoob@sc.uobaghdad.edu.iq**

ABSTRACT

This study was aimed to demonstrate the biosynthesis procedure of iron oxide nanoparticles (Fe_2O_3 NPs) by using prodigiosin pigment produced from environmental isolate *Serratia marcescens* as a reducing and stabilizing agent. Additionally, the synthesis conditions were precisely taken into consideration as a pH of 7 and a temperature of 50°C alongside a concentration of prodigiosin of 12 mg/ml with a precursor of ferric sulfate of 5 mg/50ml in deionized distilled water (DDW). Biosynthesized Fe_2O_3 nanoparticles have presented many applications such as catalysis, biosensing, anticancer, and biomedical, etc. The study of optimum condition for the synthesis of Fe_2O_3 was characterized by different techniques, such as (XRD, UV-VIS, AFM, FTIR and FE-SEM). The wavelength of biosynthesis of Fe_2O_3 by using UV-VIS is (284 nm), Image FE-SEM displays Spherical Fe_2O_3 NPs in nano-cluster form and the average volume is (35.01) nm). And the effect of Fe_2O_3 NPs on bacteria *Enterococcus faecalis* on an inhibition zone 31 mm.

Key Words: Fe_2O_3 NPs, Antimicrobial activity, biosynthesis nanoparticles, biological pigment..

تقييم التأثيرالبيولوجي لدقائق اوكسيد الحديد النانوي المصنع على بكتريا *Enterococcus faecalis*

رحمة ماجد كامل ليث احمد يعقوب
باحث استاذ مساعد

المستخلص

هدفت الدراسة الحالية الى تصنيع الدقائق النانوية بالطريقة البايولوجية وباستخدام صبغة البرودجيوسين المنتجة من العزلة البيئية لبكتريا *Serratia marcescens* كعامل مختزل ومثبت لدقائق الحديد النانوية. بالإضافة إلى ذلك ، تم أخذ ظروف التركيب في الاعتبار على وجه التحديد باعتبارها درجة حموضة 7 ودرجة حرارة 50 °C درجة مئوية جنبًا إلى جنب مع تركيز برورديجيوسين 12 mg/ml مع سلائف الحديد 5mg/50ml في الماء المقطر منزوع الأيونات حيث تمتلك دقائق الحديد النانوية المصنعة بالطريقة الحيوية عده استعمالات طبية حياتية مثل مضادة للخلايا السرطانية، التحسس الحيوي، محفزات وغيرها. تم دراسة الظروف المثلى لتصنيع دقائق الحديد النانوية وقد تم الكشف عنها باستخدام تقنيات متعددة منها (UV–VIS, XRD, AFM, FTIR, FE–SEM) وقد كان الطول الموجي لدقائق الحديد النانوية بأستخدام ال UV–VIS (284)واظهرت نتائج ال FE–SEM ان دقائق التيتانيوم النانوية تكون كروية الشكل وكان معدل حجم الدقائق النانوية (nm35,01) باستخدام الـ AFM. وان تاثير الحديد النانوي على بكتريا *Enterococcusfaecalis* بتثبيط نمو بكتيري هو 31 ملم.

الكلمات المفتاحية: دقائق الحديد النانوية ،الطريقة البايولوجية , فعالية مضادة للبكتريا, صبغة البرودجيوسين

Received:27/12/2020, Accepted:1/3/2021

INTRODUCTION

Enterococcus the Gram-positive bacterium *E.faecalis* is one of the human and animal gastrointestinal flora. They even reside in the mouth and the vagina They are very robust so that they can live in humid, salty, or acidic environments (13). This type of bacterium is characterized using the Vitek-2 system, polymerase chain reaction (PCR), and biochemical tests. Specifically, Bacteria *E. Faecalis* may even be susceptible to severe human and animal diseases, such as endocarditis, meningitis, intra-abdominal and urinary tract also some other infections(30). *E. faecalis*), a bacterium of the lactic acid and a com *E. Faecalis* is a Gram-positive spherical or ovoid cell that exists in pairs or chains of individuals. Similar length. The species is negative in catalase reaction, though it can sometimes occur Produce a pseudo catalase when grown on media containing blood However the reaction is simple, and therefore easy to overlook. (10). This bacterial species has emerged as a significant cause of worldwide hospital-acquired infections. Some genotypes are particularly adapted to the healthcare facility, and this adaptation has recently been linked to the enrichment of mobile genetic elements, including prophages, (31). Nanoparticles and nano-biomedicine is the capacity to calculate, show, manipulate and produce items on an atomic scale, recurrently between (1 – 100) nanometers. Now a day's electronic device efficiency and minimization is very important compared to other parameters in which nanomaterials play a very important role. Everyone is focused on nanotechnology because of its vast of applications in almost all types of industries from textiles to medicine including its activity as antibacterial, the most significant aspect of which is the wide use of nanostructures in mechanics, optics, electronics, biotechnology, microbiology, environmental remediation, medicine, various engineering and material sciences (1,33). The use of environmentally benign raw material such as Biological (Bacteria) extracts for the synthesis of iron oxide nanoparticles provides several economic and compatible advantages For drug companies and therapeutic targets, since they prevent to use of toxic chemicals for the manufacturing protocol (1, 5). Chemical synthesis methods contribute to the presence of some toxic chemicals that could have harmful effects in medical applications Biological synthesis of metallic nanoparticles by bacteria, extracts are at present render exploitation as some research work on it (6, 7, 13). Biological systems, such as bacteria, contain macromolecules, most of these are in the nanometer range (7). Cellular extraction from these bacterial species is used to produce nanoparticles of various sizes and Biological compositions (7) The components present in the bacteria extracted are responsible for the reduction of iron Acceptable substrates, such as ferric sulfate, can also be used to reduce bacteria extracts (9, 13). Biological nanotechnology has a great deal of interest and involves a wide variety of processes that minimize or remove harmful substances. to preserving the environment. Biological production supplies more advantages than chemical methods and physical methods since it is simple to process, very cost-effective and scalable for large-scale production (10 ,26). For biological and medical specialty applications, magnetic iron oxide nanoparticles are the first choice due to their biocompatibility, superparamagnetic behavior and chemical stability.(15) Numerous studies, like that of Ramezani on) studied results|the consequences|the results of iron chemical compound nanoparticles concentrations on other bacteria. They show that the 30 µg/ml super magnet iron oxide nanoparticles (SIONPs) reduced biofilm biomass in 11 isolates. Jehan determined the Anti-biofilm effect of Fe2O3 NPs on coated catheters against S. aureus and E.coli. The results obtained from the Fe2O3 NPs were recorded; the utmost biofilm inhibition was 33.97% against S. aureus, followed by 16.92% occurred against E.coli. Another study reportable the stimulatory effect of SIONPs at 5 mg/ml on biofilm formation in gram-negative *(P. aeruginosa* and *E. coli*) and Gram-positive (E.faecalis and B. subtilis) bacterium used different concentrations of Fe2O3NPs and ended that the iron nanoparticles have negligible toxicity on the living bacteria cells. They were found to be applicable in numerous components of

biotechnology fields. Namasivayam determined the reduction in carbohydrates and proteins of a biofilm matrix derived from S.aureus on a coated tube when being treated with nanoparticles. In a study by Taylor and Webster, it had been shown that 12 hrs treatment of Iron oxide NPs was done at 10 µg/ml as a multifunctional platform to disrupt S.epidermidis colony assembly and forestall biofilm formation. (2,5,27). This study was aimed; the purified prodigiosin from *Serratia marcescens* was used to biosynthesize iron oxide nanoparticles as a reducing and stabilizing agent. As well as the potential application of the synthesized nanoparticles in vitro as an antibacterial activity against human pathogenic bacteria (*Enterococcus faecalis*) was studied (25).

MATERIALS AND METHODS

Bacterial isolation

In this study, the isolated bacteria *Enterococcus faecalis* were collected from Septemper 2019 to january 2020 from three different hospitals namely, Al-Yarmouk, and Baghdad/Medical city; Alwiya Maternity hospital, this includes 226 clinical specimens' comparison concerning urine and vaginal swab and stool. The collected specimens were directly streaked on Bileesculinagar (11). incubated at 37 ˚C for 24 hours. On Bail escolin agar, they were black colonies, shown in figure.1 Other identification tests included Biochemical tests and morphological characteristics were performed (7, 8), and identification using automated methods (Vitek II system) shown in Figure 1.

Figure 1. *Enterococcus faecalis* on Bile esculin agar

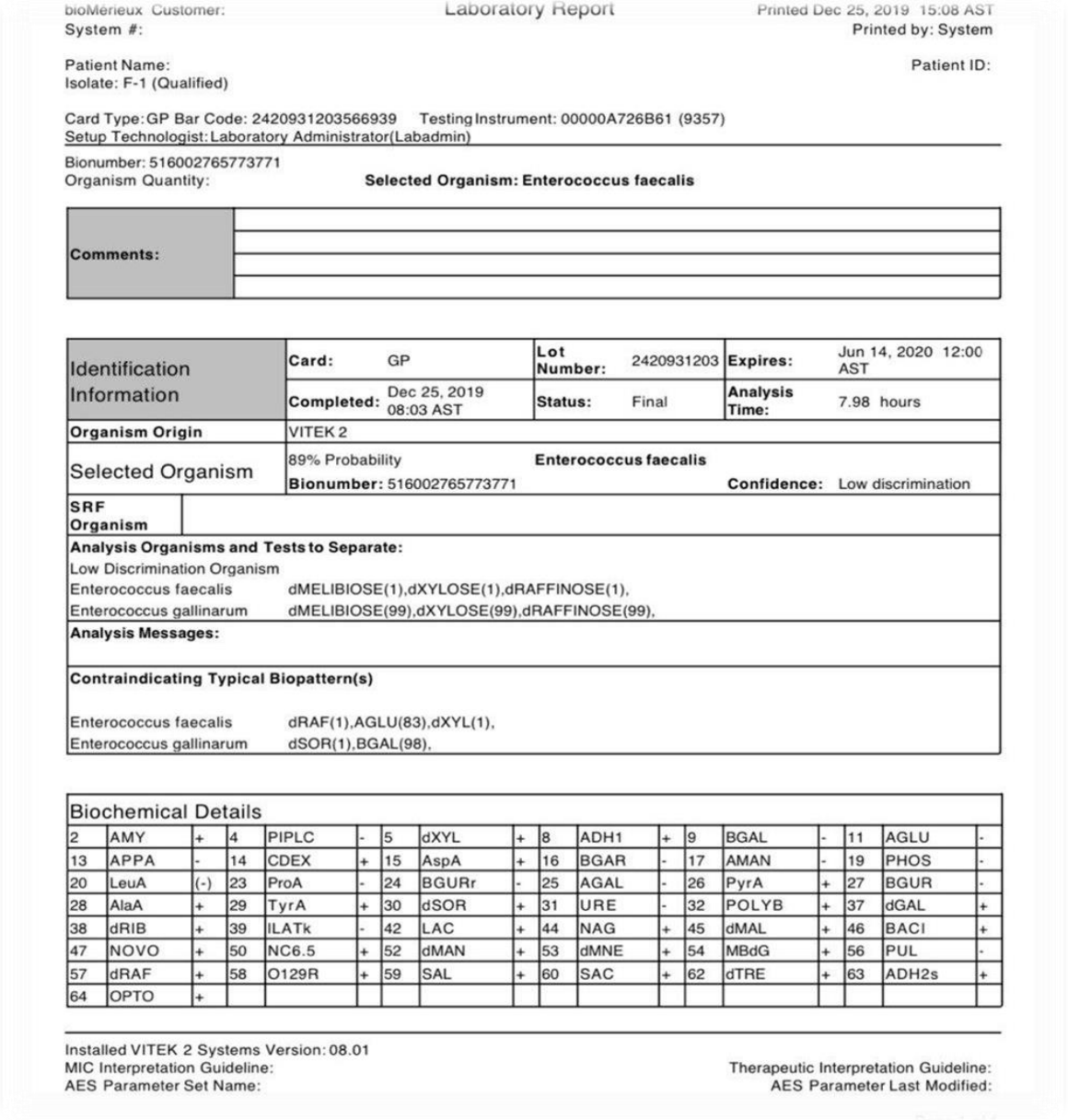

bioMérieux Customer: Laboratory Report Printed Dec 25, 2019 15:08 AST
System #: Printed by: System

Patient Name: Patient ID:
Isolate: F-1 (Qualified)

Card Type: GP Bar Code: 2420931203566939 Testing Instrument: 00000A726B61 (9357)
Setup Technologist: Laboratory Administrator(Labadmin)

Bionumber: 516002765773771
Organism Quantity: **Selected Organism: Enterococcus faecalis**

Comments:	

Identification Information	**Card:** GP		**Lot Number:** 2420931203	**Expires:**	Jun 14, 2020 12:00 AST
	Completed: Dec 25, 2019 08:03 AST		**Status:** Final	**Analysis Time:**	7.98 hours
Organism Origin	VITEK 2				
Selected Organism	89% Probability	**Enterococcus faecalis**			
	Bionumber: 516002765773771			**Confidence:**	Low discrimination
SRF Organism					

Analysis Organisms and Tests to Separate:
Low Discrimination Organism
Enterococcus faecalis dMELIBIOSE(1),dXYLOSE(1),dRAFFINOSE(1),
Enterococcus gallinarum dMELIBIOSE(99),dXYLOSE(99),dRAFFINOSE(99),

Analysis Messages:

Contraindicating Typical Biopattern(s)

Enterococcus faecalis dRAF(1),AGLU(83),dXYL(1),
Enterococcus gallinarum dSOR(1),BGAL(98),

Biochemical Details

2	AMY	+	4	PIPLC	-	5	dXYL	+	8	ADH1	+	9	BGAL	-	11	AGLU	-
13	APPA	-	14	CDEX	+	15	AspA	+	16	BGAR	-	17	AMAN	-	19	PHOS	-
20	LeuA	(-)	23	ProA	-	24	BGURr	-	25	AGAL	-	26	PyrA	+	27	BGUR	-
28	AlaA	+	29	TyrA	+	30	dSOR	+	31	URE	-	32	POLYB	+	37	dGAL	+
38	dRIB	+	39	ILATk	-	42	LAC	+	44	NAG	+	45	dMAL	+	46	BACI	+
47	NOVO	+	50	NC6.5	+	52	dMAN	+	53	dMNE	+	54	MBdG	+	56	PUL	-
57	dRAF	+	58	O129R	+	59	SAL	+	60	SAC	+	62	dTRE	+	63	ADH2s	+
64	OPTO	+															

Installed VITEK 2 Systems Version: 08.01
MIC Interpretation Guideline: Therapeutic Interpretation Guideline:
AES Parameter Set Name: AES Parameter Last Modified:

Figure 1. Vitek II for *Enterococcus faecalis*

Prodigiosin pigment production: In a typical procedure, Fermentation media Preparation is based on (15). Medium prepared by mixing components such as Peptone (5 g/L) as nitrogen, source sucrose (10 g/L) as carbon source, $MgSO_4.7H_2O$ (0.61 g/L), $MnSO_4.4H_2O_2$ (2 g/L), $CaCl_2.2H_2O$ (8.82 g/L) and $FeSO_4.4H_2O$ (0.33 g/L). The PH was set to 7.0 and then sterilized at 121° C for 15 minutes by autoclaving. After sterilization, the medium left to cool and inoculated 2% of the selected bacteria isolate (selected bacteria isolate a 0.5 McFarland standard corresponds to 1.5×10^8 CFU/ml) And cultured in a shaker incubator at 28 °C for 48 hours at 120 Revolutions per minute rpm (9).

Extraction and purification of Prodigiosin pigment: The Raw prodigiosin has been isolated from250 ml of *S.marcescens* cell-free broth culture obtained after 1 hours of incubation. The culture medium was centrifuged at 8000 rpm for 15 minutes. The supernatant was discarded and 250 ml of methanol was added to the harvested cell and thoroughly mixed at room temperature for 3 hours. The resulting mixture was then centrifuged for 20 min at 8000 rpm, collecting and filtering the supernatant through a filter paper (0.2 µm, Whitman). A rotary evaporator was used to concentrate the methanol filtrate at 70˚C and twice the amount of chloroform was then added to extract the red pigment. The two solvents were mixed vigorously in a reparatory funnel. Chloroform phase (organic phase) was collected and dried at 45 ˚C. The resulting pigment was then dissolved in a small amount

of methanol and stored in a dark bottle in a refrigerator for antimicrobial tests and for further use (4).

Synthesis of iron oxide nanoparticles

Fe2O3 nanoparticles were synthesized via the biological synthesis approach using Ferric Sulfate $Fe_2(SO_4)_3$ (Indian) used in the preparation of nanoparticles of iron oxide Method of synthesis is done by two solutions: Solution (A) is prepared as follows: 5 gm of Ferric Sulfate $Fe_2(SO_4)_3$ in 50 ml deionized distilled water DDW dispersed by ultra-sonication bath for 30 minutes. Also, solution (B) was prepared by dissolving 10 gm/ml from prodigiosin and dispersed by ultra-sonication bath for 60 minutes. Then adjusted at PH (7.0) and then left overnight in the darkroom. The solution contains iron oxide nanoparticles, was separated and concentrated for 30 minutes by centrifugation at 6000 rpm and washed twice by deionized distilled water DDW and also precipitated for 30 minutes by centrifugation at 6000 rpm. Then dried in the oven at 60 ˚C for 30 minutes to obtain a yellow powder, and kept in dark vial. (novel)

Antibacterial test (in vitro): The antibacterial activities of the biologically synthesized Fe2O3 nanoparticles against Gram-Positive *E.faecalis* were tested using the agar well diffusion technique in which the minimal inhibition concentration (MIC) of ZnO nanoparticles was estimated (6). Herein, Müller Hinton agar sterilized medium (25 ml) was added into the sterilized Petri dishes and allowed to solidify at laboratory conditions overnight. The grown test species were extended on the agar medium through the sterile cotton swab technique. Consequently, variety of Fe2O3 concentrations (5, 10, 20, 40, 80, 160, and 320) µg/ml were poured into the pre-made wells. The attained plates were then inoculated for 24 hrs. at a temperature of 37 °C. Hereinafter, the zone of inhibitions was measured around the pre-made wells (6, 16, 18, 32)

RESULTS AND DISCUSSION

Production of prodigiosin pigment

The production of prodigiosin started after 12 hrs. of shaker incubator. At the end of the exponential phase (at 48 hrs. of incubation), the concentration of prodigiosin was approximately 0.71 g/L (after four runs)and reached its maximum of 0.83 g/L during the stationary phase after 45 hrs. Of shaker incubator. During the incubation, the color of the medium turned gradually end of the exponential phase (at 48 hrs. of incubation), the concentration of prodigiosin was approximately 0.71 g/L (after four runs)and reached its maximum of 0.83 g/L during the stationary phase after 45 hrs. Of shaker incubator. During the incubation, the color of the medium turned gradually red as a result of the production of prodigiosin which accumulated mainly during the stationary phase (20).

Characterization of prodigiosin pigment

The prodigiosin developed by *Serratia marcescens* is characterized by scanning a UV-visible spectrophotometer (Shimadzu, Japan) to detect the maximum absorption. Absorbance is measured at 529 nm (31). As shown in figure 2.

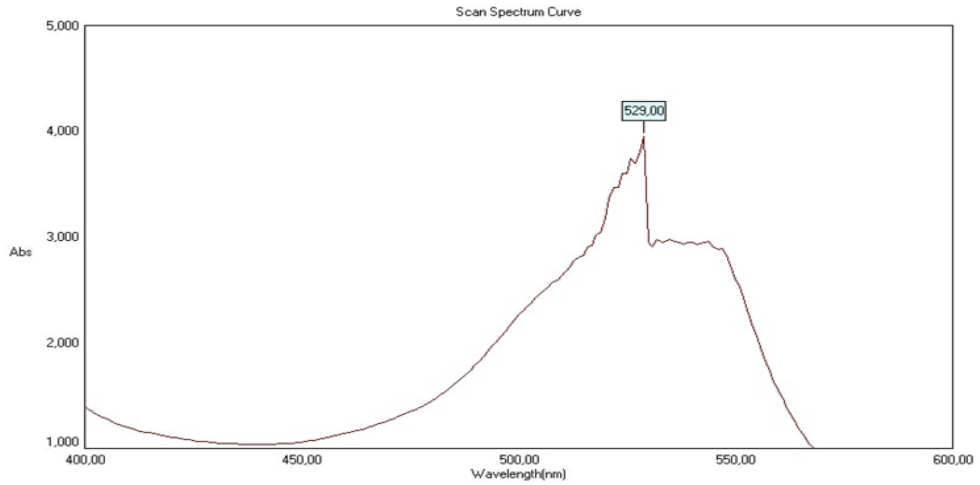

Figure 2. Absorption pattern of purified pigment, isolated from *Serratia* sp. Absorbance is measured 529 nm

Atomic force microscopy (AFM)

The surface shape formation of the Fe_2O_3 NPs was studied by atomic force microscopy to show that Fe_2O_3 NPs 2D and 3D(24). (Fig 2). AFM images show that the synthesized Fe_2O_3 NPs are spherical. The size of an average diameter of 35.01 nm was also measured by AFM Fig 3**.**

Sample:Fe_2O_3	**Code:Sample Code**
Line No.:line 1	**Grain No.:633**
Instrument:CSPM	**Date:2019-11-18**
Avg. Diameter:35.01 nm	**<=10% Diameter:16.00 nm**
<=50% Diameter:30.00 nm	**<=90% Diameter:58.00 nm**

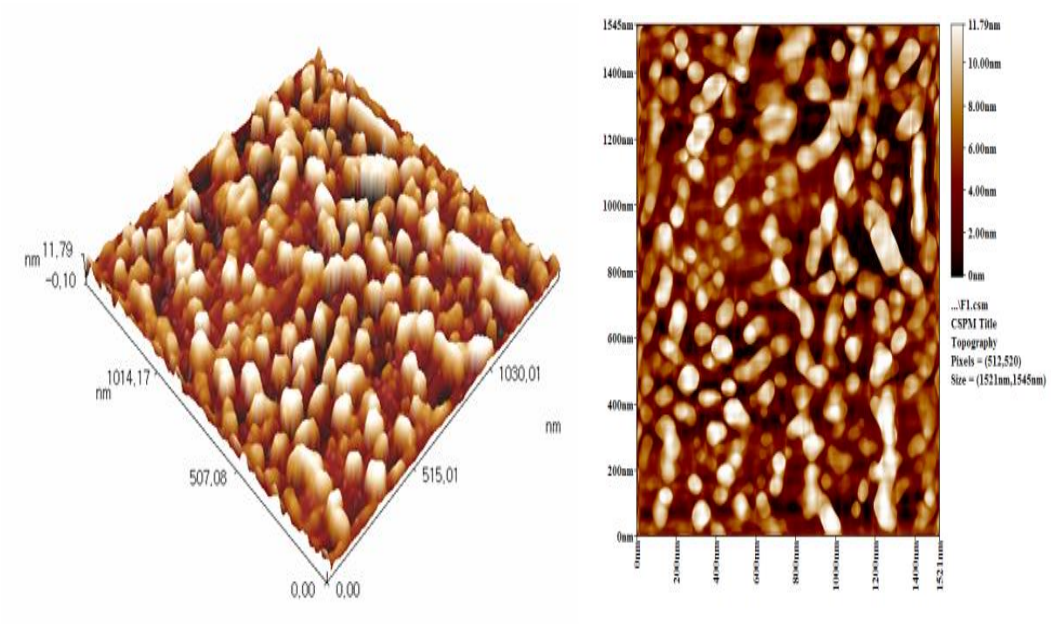

3D **2D**

Figure 3. Average size of Fe_2O_3 NPs Synthesized using Prodigiosin illustrate 2D and 3D topological by (AFM)

X-Ray Diffractometer

The X-ray deviation examination was performed to define the surface morphology and the composition of the crystals Of Fe_2O_3 NPs, including crystalline size, lattice parameters, the thickness of the crystal, and textile factor. X-ray deviation results for the Fe_2O_3 model were calibrated to the typical datum of the Joint Committee Powder Diffraction Standard (JCPDS) No. 11-0614. The X-ray diffraction test results of the Fe_2O_3 NP include data format of an angle of deviation and strength of deviation. The deviation model was plotted by use Origin 9.0 for the windows operating system, in Figure 4 The deviation pattern suggests that: presence of seven diffraction peaks. Seven diffraction peaks indicate the electron diffraction process that occurs in the diffraction plane of Fe_2O_3 nanoparticles, namely fields (220), (311), (400), (422), (511), (440) and (533), which are characteristics of the Fe_3O_4 nanoparticle diffraction pattern according to JCPDS standard data. 11-0614 (14, 17). As the width of the peak increases the particle size decreases, which is similar to that of nanomaterial. We obtained the Crystalline structure parameter b=0.3785 nm and c=0.9513 nm. The average diameter of crystallite was calculated by the equation of Debye-Scherrer as. (32). The result revealed that there exists eight-strong different diffraction peaks corresponding to the crystal planes of crystalline Fe_2O_3 NPs observed at 2θ (θ=diffraction angle) values of 30.10°, 35.51°, 45.21°, 53.44°, 57.31°, 62.81°.

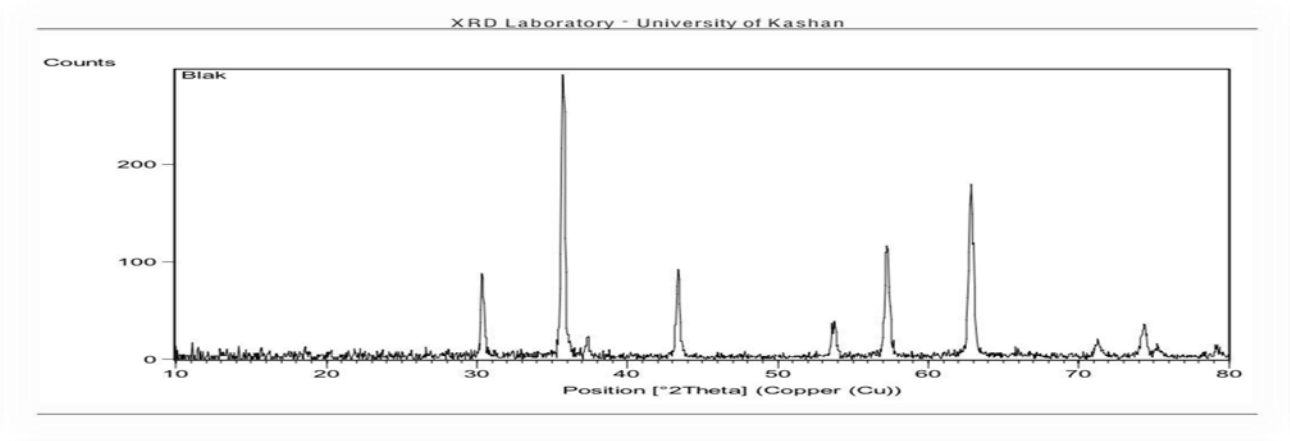

Figure 4. XRD Pattern of Fe_2O_3 Nanoparticles

Fourier transform infrared (FTIR) Spectroscopy analysis

FTIR spectrum has determined the functional groups of nanoparticles. (Fig. 5) Represents the absorption spectrum of Biologically synthesized nanoparticles in FTIR. An intense peak at 3398.34 cm^{-1} was visible due to OH stretching mode. The occurrence of the peak properties at 1629.74 cm^{-1} suggested the presence of crystallographic H_2O molecules, i.e. O–H bend. The wide peak at 455,17 cm^{-1} and 572,82 cm^{-1} respectively represented the Fe–O band and Fe–O–Fe skeletal frequency (24).

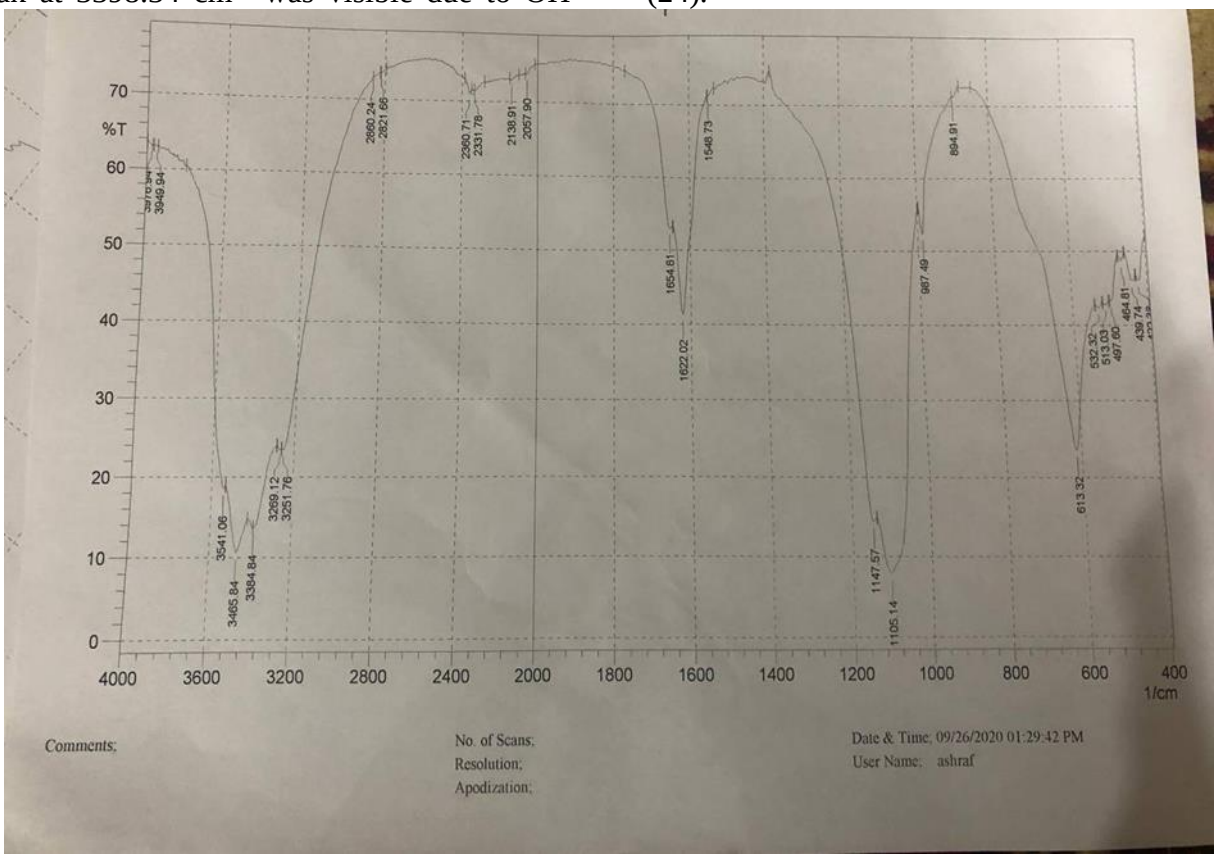

Figure 5. FTIR Images of $Fe_2(SO_4)_3$

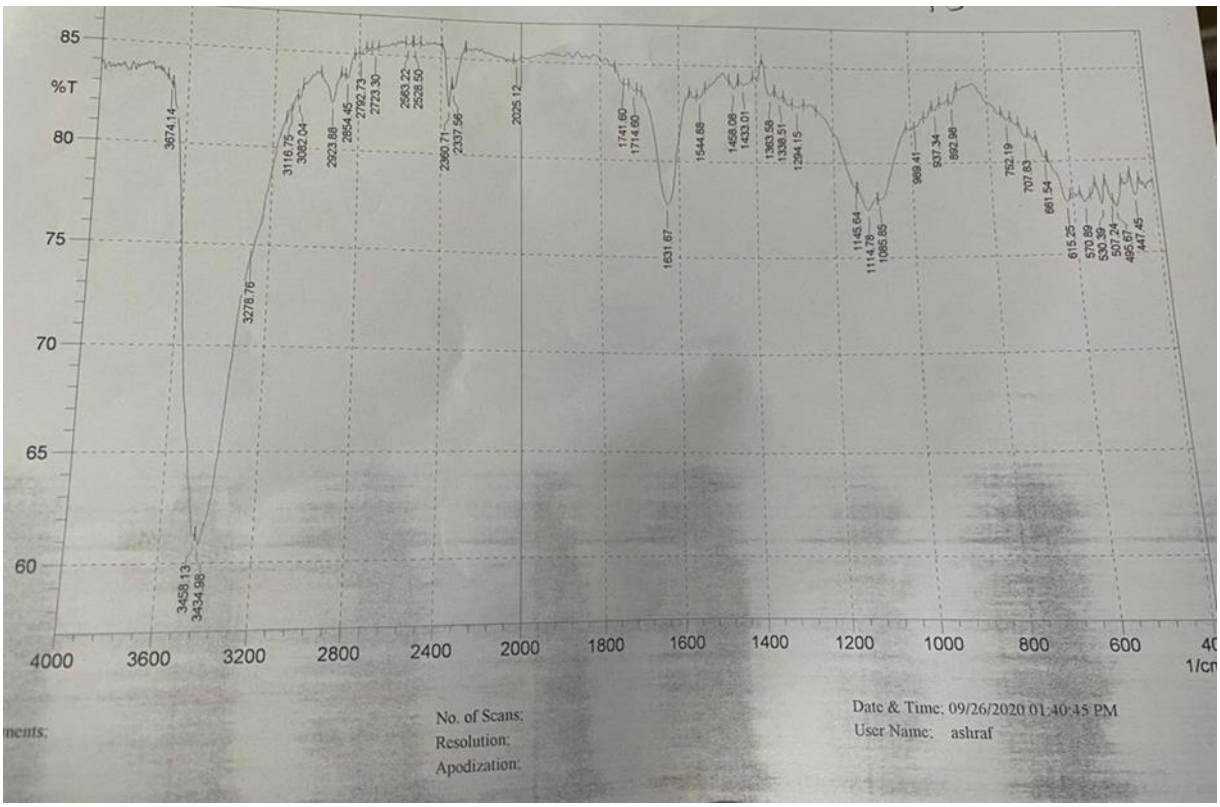

Figure 6. FTIR Images of of prodigiosin

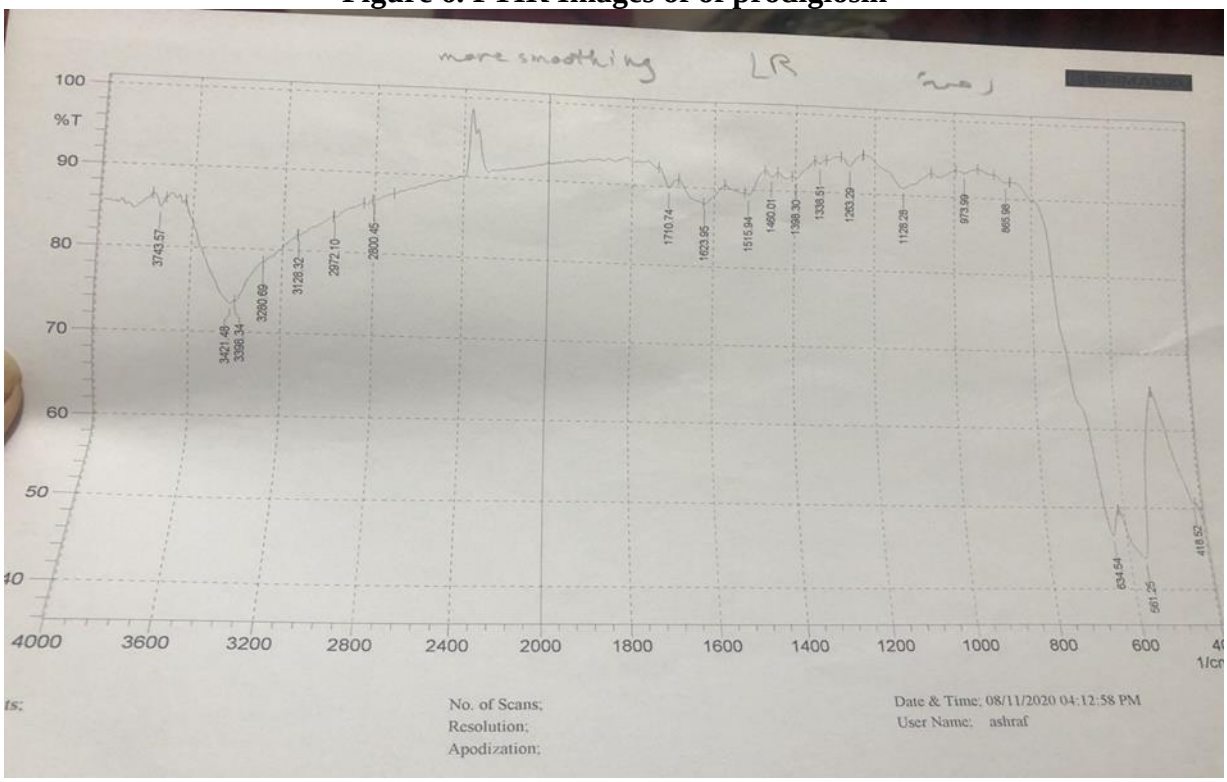

Figure 7. FTIR Images of Fe_2O_3 Synthesized using Prodigiosin

Field emission scanning electron microscopy

Through applying FE-SEM, images were taken of the sample at A magnification of 50kx. Focused on (Fig . 7) the whole sample has soft planes and a uniform shape in the form of Fe_2O_3 nanocluster centers. It has been investigated that the particle size increases with a rise in calcination temperature due to the agglomeration of smaller particles at high temperatures. Low temperatures lead to better connections between nanoparticles As a consequence, the form of the NPs has changed into a sphere (24, 29).

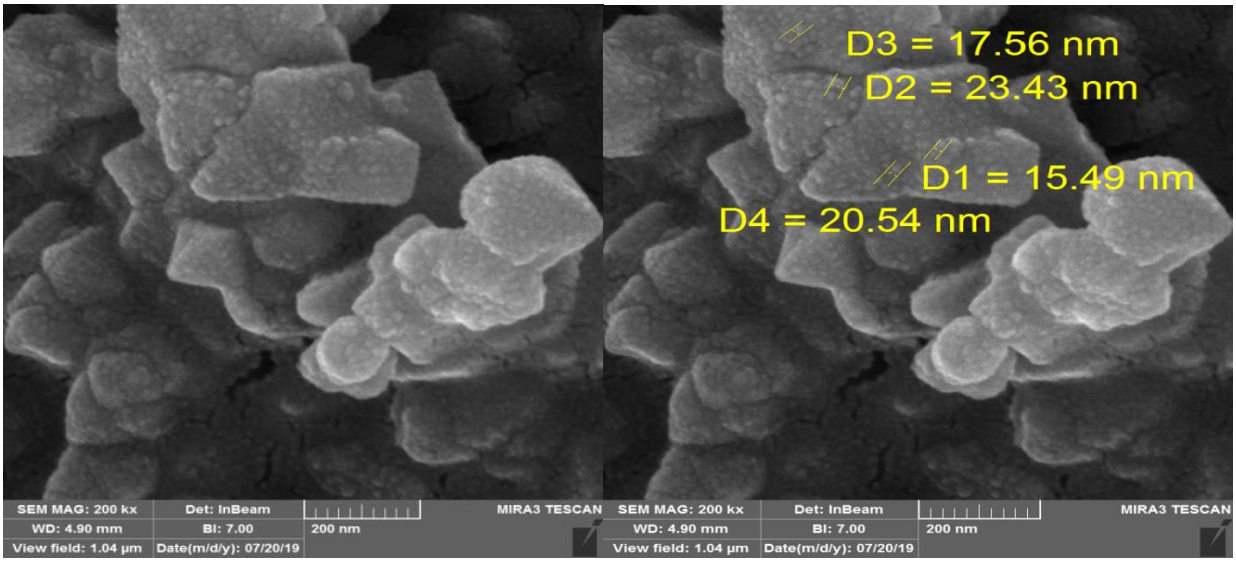

Figure 8. FE-SEM Images of Fe_2O_3 NPs Synthesized using Prodigiosin

Antibacterial test (in vitro)

Fe_2O_3 NPs antibacterial activity was investigated using gram-Positive bacteria (*Enterococcus faecalis*) collected from the medical city, Baghdad. The minimal inhibition concentration (MIC) of Fe_2O_3 NPs for microorganisms was calculated by the use of the agar well diffusion technique (5, 16). Almost 25 ml of the Mueller Hinton agar sterilized medium was placed into sterile plates and Enabled to solidify at room temperatures. The growth of the test species was transported and spread over The agar medium by a sterile cotton swab separately, wells were made. Subsequently, Diverse ratios of Fe_2O_3 NPs (5, 10, 20, 40, 80, 160, 320,) µg / ml. Plates inoculated with Fe_2O_3 NPs were incubated at °C for 24 hours, The inhibition zone around the well was assessed after incubation (14, 23) Results of Fe_2O_3 NPs antibacterial activity were demonstrated in (Fig. 8). The antibacterial activity was found to be directly dependent upon the Fe2O3 NPs concentration. Table 2 shows that the maximum inhibition zones of *Enterococcus faecalis.* were 31 mm respectively at concentration 320 µg/ml of Fe_2O_3 NPs, Whereas the minimum inhibition, zones were located at 5 µg / ml Fe_2O_3 NPs concentrations. The difference in inhibition diameter may be due to different interactions between Fe_2O_3 NPs and the microorganism, and due to the susceptibility of bacteria used in the current study. The main mechanism of toxicity of Fe_2O_3 NPs potentially associated with metal oxides carries the positive charge even though the microorganisms bear negative charges; this results in electromagnetic interaction between microorganisms and metal oxides leading to oxidation and finally death of microorganisms The MIC was determined over a range from 5 to 320 µg/mL by the serial dilution method, as described CLSI (17). The bactericidal action of Fe_2O_3 nanoparticles on bacteria is of extreme importance due to the ability of pathogenic bacteria to join the food chain of the ecosystem (28). The antimicrobial effect of Fe_2O_3 against fungi and bacteria has been demonstrated (23, 28) and communicating in modern research.

Table 1. Inhibition zone of Fe2O3 nanoparticles

	Fe2O3 concentration (µg/mL)	Inhibition zone (mm)
A	**5**	**Nill**
B	**10**	**8**
C	**20**	**13**
D	**40**	**16**
E	**80**	**22**
F	**160**	**26**
G	**320**	**31**

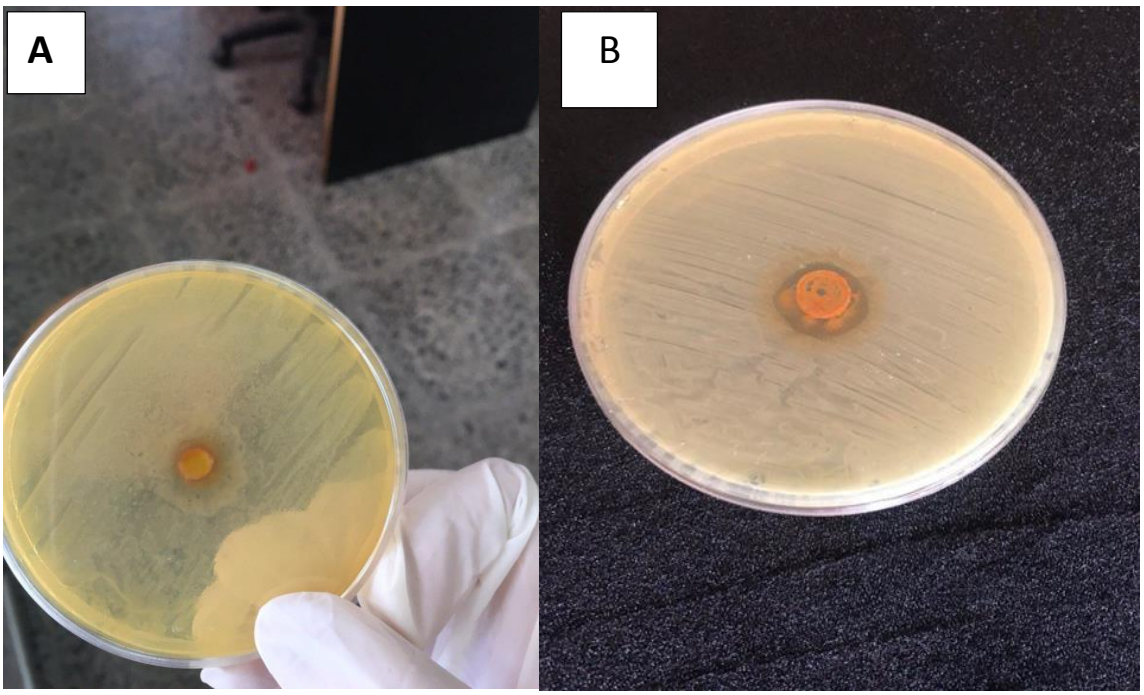
A
B

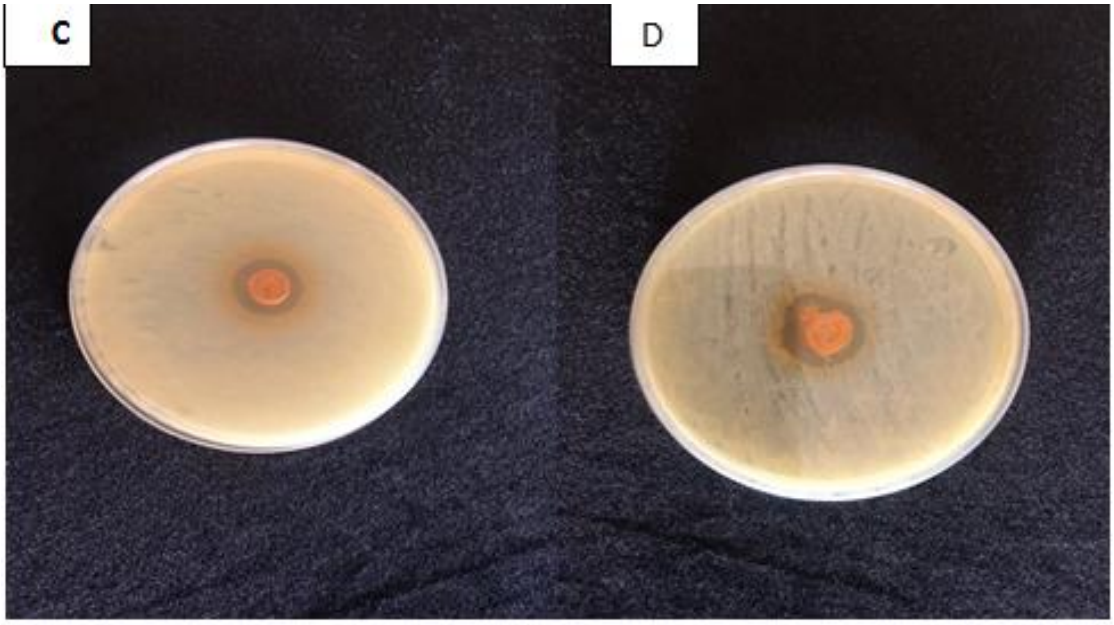
C
D

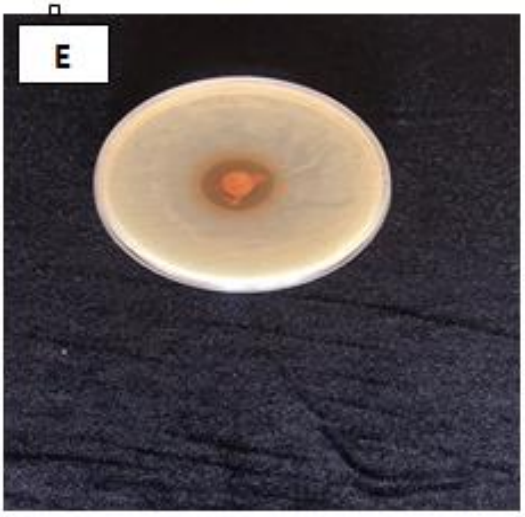
E

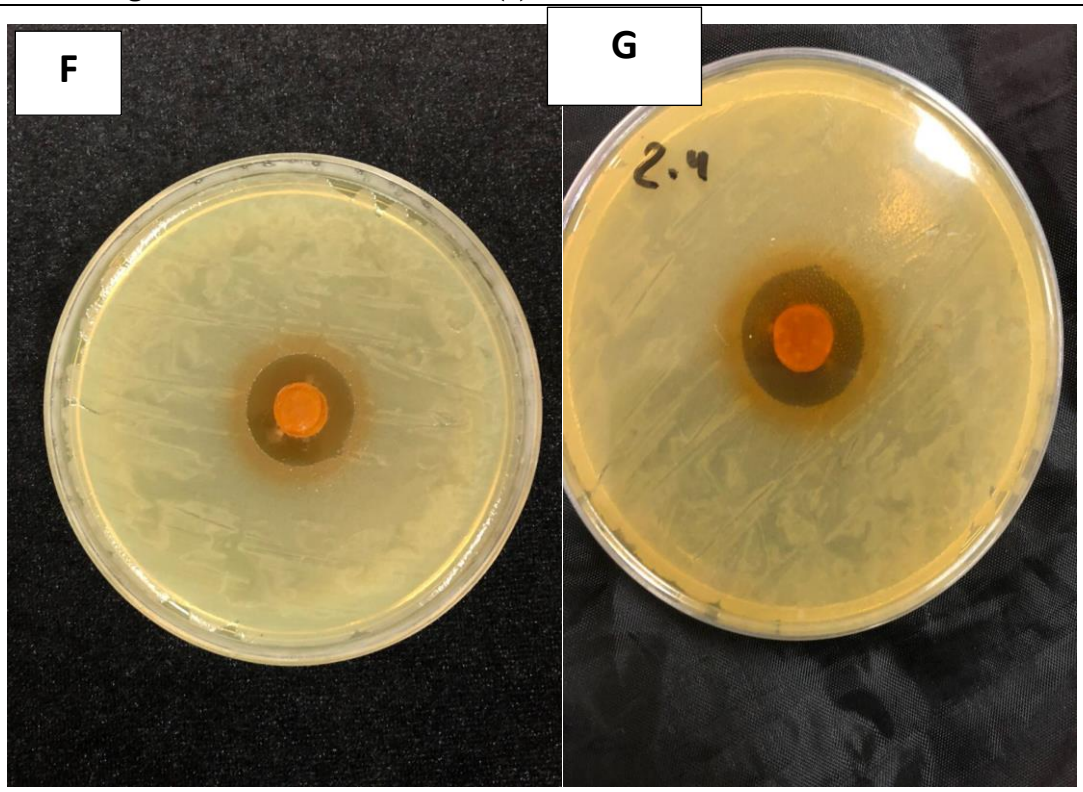

Figure 9. Antibacterial activity of the bio-synthesized Fe_2O_3 nanoparticles against *E.faecalis* at concentration of (a) 5, (b) 10, (c) 20 (d) 40, (f) 80, (g) 160 and (e) 320µg/ml.

CONCLUSION

In this study, the biosynthesis of Fe_2O_3 nanoparticles using prodigiosin as a reducing agent was demonstrated successfully. Additionally, the attained Fe_2O_3 NPs were characterized using UV-Vis, AFM, XRD, FT-IR, and FE-SEM. Techniques. In particular, The XRD patterns showed the successful Fe_2O_3 NPs phase formation, while the FE-SEM demonstrated that the prepared Fe_2O_3 NPexhibited spherical particles as well as plate-like structures with an average diameter size ranging between 30-50 nm. While the AFM revealed an average diameter of 35.01 nm. In the antibacterial activity test, it was found that the bio-synthesized has a strong antibacterial activity against the introduced bacteria. The maximum inhibition zone was found to be 31 mm at a concentration of 320 µg/mL.

REFRENSES

1. Al-Azawi, M. T., S. M. Hadi, and C. H. Mohammed, 2019. Synthesis of silica nanoparticles via green approach by using hot aqueous extract of Thuja orientalis leaf and their effect on biofilm formation. The Iraqi Journal of Agricultural Sciences, 50, 245-255

2. AL-Mousawi, H. T., M. I. Al-Taee, M. N. Rasheed, and Q. N. Al-Hajjar, 2019. Molecular and nanotechnical study for antibiofilm formation and csuE gene expression activities of synthesized iron oxide nanoparticles against multidrug-resistant acinetobacter baumannii isolates. Iraqi Journal of Biotechnology, 18(2), 201-2015

3. Awwad, A. M., and N. M. Salem, 2012. A green and facile approach for synthesis of magnetite nanoparticles. Nanoscience and Nanotechnology, 2(6), 208-213

4. Chen, W. C., W. J. Yu, C. C. Chang, J. S. Chang, S. H. Huang, C. H. Chang,... and Y. H. Wei, 2013. Enhancing production of prodigiosin from Serratia marcescens C3 by statistical experimental design and porous carrier addition strategy. Biochemical Engineering Journal, 78, 93-100

5. Christian, P., F. Von der Kammer, M. Baalousha, and T. Hofmann, 2008. Nanoparticles: structure, properties, preparation and behaviour in environmental media. Ecotoxicology, 17(5), 326-343

6. Das, A. K., A. Marwal, and R. Verma, 2014. Datura inoxia leaf extract mediated one step green synthesis and characterization of magnetite (Fe3O4) nanoparticles. Research and Reviews: Journal of Pharmaceutics and Nanotechnology, 2(2), 21-24

7. Edwards, P. R., and W. H. Ewing, 1972. Identification of enterobacteriaceae. Identification of Enterobacteriaceae., 3rd ed pp:245.

8. Facklam, R. R. 1973. Comparison of several laboratory media for presumptive identification of enterococci and group streptococci. Applied microbiology, 26(2), 138-145

9. Forbes, B. A., D. F. Sahm, and A. S. Weissfeld, 2007. Bailey and Scotts' Diagnostic microbiology 12th. ed. St Louis, Mosby

10. Fortina, M. G., G. Ricci, D. Mora, and P. L. Manachini, 2004. Molecular analysis of artisanal Italian cheeses reveals Enterococcus italicus sp. nov. International Journal of Systematic and Evolutionary Microbiology, 54(5), 1717-1721

11. Harwood, V. J., N. C. Delahoya, R. M. Ulrich, M. F. Kramer, J. E. Whitlock, J. R. Garey, and D. V. Lim, 2004. Molecular confirmation of Enterococcus *faecalis* and E. *faecium* from clinical, faecal and environmental sources. Letters in applied microbiology, 38(6), 476-482

12. Khanafari, A., M. M. Assadi, and F. A. Fakhr, 2006. Review of prodigiosin, pigmentation in Serratia marcescens. Online Journal of Biological Sciences, 6(1), 1-13

13. Liu, J., S. Z. Qiao, Q. H. Hu, and G. Q Lu,. 2011. Magnetic nanocomposites with mesoporous structures: synthesis and applications. small, 7(4), 425-443

14. Machado, I., J. Graça, H. Lopes, S. Lopes, and M. O. Pereira, 2013. Antimicrobial pressure of ciprofloxacin and gentamicin on biofilm development by an endoscope-isolated Pseudomonas aeruginosa. International Scholarly Research Notices, 2013

15. Mahdavi, M., M. B. Ahmad, M. J. Haron, F. Namvar, B. Nadi, M. Z. A. Rahman, and J. Amin, 2013. Synthesis, surface modification and characterisation of biocompatible magnetic iron oxide nanoparticles for biomedical applications. Molecules, 18(7), 7533-7548

16. Mahdavi, M., F. Namvar, M. B. Ahmad, and R. Mohamad, 2013. Green biosynthesis and characterization of magnetic iron oxide (Fe3O4) nanoparticles using seaweed (*Sargassum muticum*) aqueous extract. Molecules, 18(5), 5954-5964

17. Malega, F., I. P. Indrayana, and E. Suharyadi, 2018. Synthesis and characterization of the microstructure and functional group bond of fe3o4 nanoparticles from natural iron sand in Tobelo North Halmahera. Jurnal Ilmiah Pendidikan Fisika Al-Biruni, 7(2), 13-22

18. Mansoori, G. A. 2005. Principles of nanotechnology: molecular-based study of condensed matter in small systems. World Scientific. pp:

19. Matos, R. C., N. Lapaque, L. Rigottier-Gois, L. Debarbieux, T. Meylheuc, B. Gonzalez-Zorn, and P. Serror, 2013. Enterococcus faecalis prophage dynamics and contributions to pathogenic traits. PLoS Genet, 9(6), e1003539

20. Mikhaylova, M., D. K. Kim, N. Bobrysheva, M. Osmolowsky, V. Semenov, T. Tsakalakos, and M. Muhammed, 2004. Superparamagnetism of magnetite nanoparticles: dependence on surface modification. Langmuir, 20(6), 2472-2477

21. Mittal, A. K., Y. Chisti, and U. C. Banerjee, 2013. Synthesis of metallic nanoparticles using plant extracts. Biotechnology Advances, 31(2), 346-356

22. Mohanpuria, P., N. K. Rana, and S. K Yadav,. 2008. Biosynthesis of nanoparticles: technological concepts and future applications. Journal of Nanoparticle Research, 10(3), 507-517

23. Nirmala, M. J., P. J. Shiny, V. I. N. I. T. A. Ernest, S. P. Das, A. Samundeeswari, A. M. I. T. A. V. A. Mukherjee, and N. Chndrasekaran, 2013. A review on safer means of nanoparticle synthesis by exploring the prolific marine ecosystem as a new thrust area in nanopharmaceutics. Int. J. Pharm. Sci, 5, 23-29

24. Pailleret, A., N. T. L. Hien, D. T. M. Thanh, and C. Deslouis, 2007. Surface reactivity of polypyrrole/ iron-oxide nanoparticles: electrochemical and CS-AFM investigations. Journal of Solid State Electrochemistry, 11(8), 1013-1021

25.Rastegari, B., H. R. Karbalaei-Heidari, S. Zeinali, and H. Sheardown, 2017. The enzyme-sensitive release of prodigiosin grafted β-cyclodextrin and chitosan magnetic nanoparticles as an anticancer drug delivery system: Synthesis, characterization and

cytotoxicity studies. Colloids and Surfaces B: Biointerfaces, 158, 589-601

26. Shameli, K., M. B. Ahmad, A. Zamanian, P. Sangpour, P. Shabanzadeh, Y. Abdollahi, and M. Zargar, 2012. Green biosynthesis of silver nanoparticles using Curcuma longa tuber powder. International journal of nanomedicine, 7, 5603

27. Sheng-Nan, S., W. Chao, Z. Zan-Zan, H. Yang-Long, S. S. Venkatraman, and X. Zhi-Chuan, 2014. Magnetic iron oxide nanoparticles: Synthesis and surface coating techniques for biomedical applications. Chinese Physics B, 23(3), 037503

28. Stoimenov, P. K., R. L. Klinger, G. L. Marchin, and K. J. Klabunde, 2002. Metal oxide nanoparticles as bactericidal agents. Langmuir, 18(17), 6679-6686

29. Suto, M., Y. Hirota, H. Mamiya, A., Fujita, R. Kasuya, K. Tohji, and B. Jeyadevan, 2009. Heat dissipation mechanism of magnetite nanoparticles in magnetic fluid hyperthermia. Journal of Magnetism and Magnetic Materials, 321(10), 1493-1496

30. Vidana, R. 2015. Origin of intraradicular infection with Enterococcus faecalis in endodontically treated teeth. Inst för odontology Dept of Dental Medicine.pp:

31. Williams, R. P., C. L. Gott,and J. A. Green, 1961. STUDIES ON PIGMENTATION of serratia marcescens V.: Accumulation of pigment fractions with respect to length of incubation time1. Journal of bacteriology, 81(3), 376

32. Zhang, L., and T. J. Webster, 2009. Nanotechnology and nanomaterials: promises for improved tissue regeneration. Nano today, 4(1), 66-80.